Spectral of analysis of hypercontraction-indused calcium oscillations in rat ip hypoxia-indused calcium waves in isolated rat heart on the subcellular level

authors

February 21, 2019

Key words: calcium waves, calcium overloading, cardiomyocytes, myocardium, ischemia, arrhytmia

1 Introduction

Spectral analysis of hypoxia-indused calcium waves in isolated rat heart on the subcellular level

И увидели там, что с течением времени частота высокочастотных волн снижается, и это в клетках которые постепенно гиперсокращаются, судя по всему..

Показано уменьшение частоты осцилляций во времени если это повреждённый клетки, которые находятся в процессе гиперсокращения являются источником осцилляций An intracellular accumulation of Ca2+ caused by a failure of the ATP-dependent mechanisms known to be the key events in myocardial damage during ischemia (Shen & Jennings, 1972b, 1972a; Nayler, 1981). In the process of damage progression functional myocardial tissue becomes Ca2+ -overloaded and then lost functionality with the properties of Ca2+ waves changing progressively over time (Minamikawa, Cody, & Williams, 1997; Hama, Takahashi, Ichihara, & Takamatsu, 1998). Now it is well acknowledged that Ca2+ -overloaded cardiomyocytes are essential substrate for arrhythmias and contractile failure, especially in acute myocardial infarct. Ca2+ dynamics at the border zones between the infarcted and non-infarcted myocardium is considered to be a key element for arrhythmogenesis (Takamatsu, 2008). In this study, we applied the method of confocal microscopy and carried out a frequency analysis of calcium oscillations in cardiomyocytes from border zone between the necrotic and healthy myocardium. For optical registration of calcium waves. (Matsuura et al., 2018)

2 MATERIALS AND METHODS

2.1 Animals

Studies were conducted in accordance with regulations of the National Committee on Bioethics of the Russian Academy of Sciences. The protocol was approved by the Ethics Committee of the Sechenov Institute of Physiology and Evolutionary Biochemistry. Experiments were performed in hearts isolated from adult Wistar male rats (N = 00; body weight 200–250 g). Animals were anesthetized with sodium Nembutal (50 kg - 1 , i.p.), and then the hearts were harvested via thoracotomy. The preparation was retrogradely perfused via the aortic cannula through with a Tyrode's solution of the following composition (mM): 140 NaCl, 1.0 MgCl2 , 4.5 KCl, 10 glucose, 1 CaCl2 and 10 HEPES. The pH of the solution was maintained at 7.4 by continuously bubbling with 95%O2/5%CO2 and temperature maintained at 37 C. Effluent was drained via a catheter placed in dish so as not to touch the heart. Myosin ATPase inhibitor, blebbistatin (10 μ M, Sigma, USA) was added to the Tyrode's solution perfusing the heart to stop heart contraction and prevent associated artifacts (Farman et al., 2008). The experiment was carried out on inbred rats weighing about 300 g. Animals were anesthetized with Nembutal (50 mg), and then the hearts were removed. Heart perfusion was performed using a modified Langendorff system. Tyrode solution with CaCl2 (1 mM/L) was used as the perfusion medium. A similar solution with the addition of the fluorescent dyes Fluo-4 (20 μ M/L) and Di-8-ANEPPS (20 μ M/L) was used for visualization of the Ca2+ waves. To investigate spontaneous Ca2+ waves in myocardium, we positioned isolated perfused heart in organ bath with thin bottom (180 μ m), left ventricle in conjunction with an oil-immersible objective lens on an inverted microscope (Leica). This combination provide sufficient depth discrimination to focus directly onto the epicardial layers and individual cells within the intact functioning organ. 1-Phenyl-1,2,3,4-tetrahydro-4-hydroxypyrrolo[2.3-b]-7-methylquinolin-4-one was obtained from Merck. To stop heart contraction (-)-blebbistatin was used (20 μ M/L). The dyes 4-(6-Acetoxymethoxy-2,7-difluoro-3-oxo-9-xanthenyl)-4' -methyl-2,2'-(ethylenedioxy)dianiline-N,N,N',N'-tetraacetic acid tetrakis(acetoxymethyl) ester, Fluo-4-AM,Tetramethylrhodamine Methyl Ester Perchlorate, TMRM, and 4-[2-[6-(dioctylamino)-2-naphthalenyl]ethenyl]-

1-(3-sulfopropyl)-pyridinium inner salt, Di-8-ANEPPS, was obtained from Thermo Fisher Scientific. To the simultaneous detection of fluorescence of Fluo-4 and TMRM we used an argon laser with a wavelength 488 nm and a power of 80% and a HeNe laser with a wavelength of 543 nm and a power of 80%. The fluorescence detection was carried out in the spectral range 493 nm – 540 nm for Fluo-4 and 552 nm – 792 nm for TMRM. Since the specific values of the background fluorescence depended on the density of the capillary network, the amount of connective tissue in the field of view, and other factors, the sensitivity of the PMT detector (gain) was selected individually each time, depending on the conditions of the survey, and was usually 600 to 800 units. changes in fluorescence intensity of Fluo-4 over time (xyt mode) were measured, a resonant scanner (8000 Hz) was used, and the diameter of the confocal pinhole was set to 100 mu m. A fluorescent signal was registered in the first layer of cardiomyocytes adjacent to the epicardial surface of an isolated heart (Fig. 1). The fluorescent signal was measured in a whole frame or in certain regions of interest (regions of interest, ROI). Spectral analysis of calcium oscillations was carried out using a fast Fourier transform. Studies were carried out on the model of an isolated working rat heart perfused by the method of Langendorff. The subepicardial layers of the myocardium were examined using an inverted Leica TCS SP5 laser scanning confocal microscope equipped with a resonance scanner and x20, x63 lenses with oil immersion. For visualization of cardiomyocytes, vascular network and connective tissue, perfusion of the hearts was performed with a solution with the addition of the fluorescent dye Di-8-ANEPPS. To visualize free Ca2 + ions, the Fluo-4 dye was used. For dyeing mitochondria, the TMRM dye was used, the fluorescence intensity of which is proportional to the value of the mitochondrial membrane potential ($\Delta\ \psi$). With the simultaneous detection of fluorescence Fluo-4 and Di-8-ANEPPS, an argon laser with a wavelength of 488 nm and a power of 80% was used to excite the fluorescence. Fluorescence detection was carried out using two photomultiplier tubes (PMT), 491nm - 581nm for Fluo-4 and 611nm - 792nm for Di-8-ANEPPS. With the simultaneous detection of fluorescence Fluo-4 and TMRM, an argon laser with a wavelength of 488 nm and a power of 80% and a HeNe laser with a wavelength of 543 nm and a power of 80% were used to excite the fluorescence. The fluorescence detection was carried out in the spectral range 493 nm-540 nm for Fluo-4 and 552nm-792nm for TMRM. Since the specific values of the background fluorescence depended on the density of the capillary network, the amount of connective tissue in the field of view, and other factors, the sensitivity of the PMT detector (gain) was selected individually each time, depending on the conditions of the survey, and was usually 600 to 800 units. For optical registration of calcium waves, changes in fluorescence intensity of Fluo-4 over time (xyt mode) were measured, a resonant scanner (8000 Hz) was used, and the diameter of the confocal pinhole was set to 100 μ m. A fluorescent signal was registered in the first layer of cardiomyocytes adjacent to the epicardial surface of an isolated heart (Fig. 1). The fluorescent signal was measured in a whole frame or in certain regions of interest (regions of interest, ROI). Spectral analysis of calcium oscillations was carried out using a fast Fourier transform. Calcium imaging with Fluo-4/AM was performed using a confocal laser scanningmicroscope(ZeissLSM510/Axiovert100M)witha40x(NA = 1.3) oil immersion objective. Fluorescence images (excited at 488 nm). The pinhole was set to 200 mm, resulting in ,2.5-mm optical slices. Amplifier gain and detector offset were adjusted such that neither saturation nor threshold cutoff occurred. The membrane structure of epicardial myocytes was analyzed in situ by confocal microscopy Leica SP5 equipped with x63 (NA = 1.4) oil-immersion lens]. The epicardial images were used to define the measurement duration= 109.6 s sampling frequency 14.29745 Hz To cite R in publications use: (Team et al., 2014) To cite package WaveletComp in publications use: (Roesch & Schmidbauer, 2014) Wavelet methodology is a reasonable choice to study periodic phenomena in time series, particularly in the presence of potential frequency changes across time. packages for wavelet analysis in R WaveletComp (version 1.1) analyzes the frequency structure of uni- and bivariate time series using the Morlet wavelet. 2 Contour lines added to the wavelet power spectrum delineate areas of high significance. Wavelet power spectrum of the series with variable period Horizontal arrows pointing to the right indicate that the two series x and y are in phase at the respective period with vanishing phase differences. Likewise, horizontal arrows pointing to the left indicate that the two series are in anti-phase; The arrows are plotted only within white contour lines indicating significance (with respect to the null hypothesis of white noise processes) at the 10% level. Cross-Wavelet power spectrum of the series with interval color key and restricted arrow area Limit the area where arrows are drawn to the region where both individual wavelet transforms of x and y show significance (set which.arrow.sig = "wt"), and avoid the artifacts of the image inFigure image - properties - установить размер пикселя... (for 094–: 455.9 mkm / 512px = 0,8904296875 Area = 318,363, x = 17.8427296118, $\approx$ 17.8 μ m analyze - tools - scale bar

3 RESULTS

Кальциевые волны Каким образом образуются кальциевые волны и какие это может иметь последствия. Солитоны В книжке (Kockskämper & Blatter, 2002) about atrial fibrillation ... Аритмия Мы решили применить вейвлет анализ частот кальциевый осцилляций.

The role of calcium in regulation of conraction. Роль кальция в регуляции сокращения. Роль кальция в возникновении аритмии. В ишемическом миокарде кальциевые волны рассматриватьются как аритмогенный субстрат. Эффект гипоксии на осцилляции кальция в эпикардиальном слое кардиомиоцитов.

In the course of myocardial observations after simultaneous staining of Di-8-ANEPPS and Fluo-4 under conditions where cardiac contractions were inhibited by blebbistatin, normal myocardial regions characterized by passage of a global calcium-ejection wave corresponding to sinus rhythm and small contractions were revealed. Tissue abbreviations were determined by averaging the Di-8-ANEPPS fluorescent signal from ten arbitrarily selected ROIs of 20 μ m x 20 μ m size (Figure 5). Also, the areas of the myocardium, located in different stages of ischemic damage, were identified. For the initial stage of damage, groups of cardiomyocytes with an increased value of [Ca2 +], in which high-frequency calcium waves were observed (Fig. 6), are characteristic. Nascent on the edge of the cell or in its middle, these waves can spread to neighboring cells (Figure 7). With a slight increase in the intracellular calcium concentration, such waves are erased by each subsequent global calcium release (Figure 11, B), and with a strong increase in [Ca2 +] in cardiomyocytes relative to the baseline observed in the normal myocardium, the global calcium release does not interfere with the formation of calcium waves (Fig. 11, B, D). The cardiomyocytes adjacent to the necrosis zone were characterized mainly by slow, damped calcium waves with a large amplitude (Fig. 8).

Fig. 1. Cardiomyocytes adjacent to the epicardial surface of the heart. Based on a series of optical sections, a three-dimensional image of a portion of the myocardium of an isolated rat heart stained with a potential dependent Di-8-ANEPPS dye. The epicardial surface of the heart is located on top. Different types of myocardial damage. Different parts of the myocardium of the rat, colored for active mitochondria (red) and free calcium ions (green). a is a normal tissue; b - groups of cells with reduced mitochondrial potential and elevated calcium content; c, d - groups of cells with necrotic striation. Optical sections of subepicardial ventricular layers. The scale segments are 100 μ m. Measurement of fluorescence intensity in the area of the myocardium stained for active mitochondria (red) and free calcium ions (green). The scale segment is 50 μm. For comparison, six ROIs of 10 μ m x 20 μ m are selected. Pixel intensity distribution histograms were constructed for each ROI.

Fig. 11. Pairwise comparison of calcium waves of cardiomyocytes located in the perinekrozic zone of the epicardial region of the ventricular myocardium of an isolated working rat heart. Fluorescence intensity curves of Fluo-4 versus time are presented. A, B - comparison of signals in neigh-

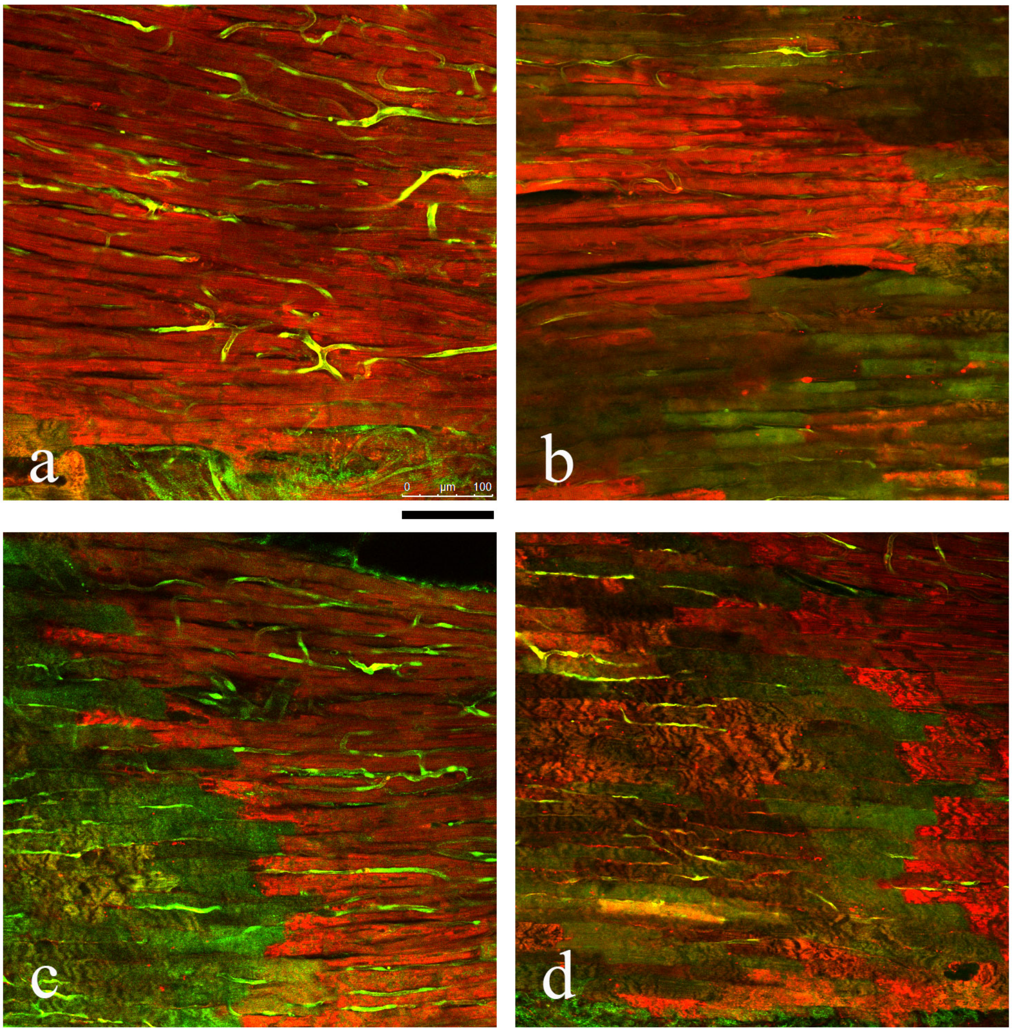

Figure 1: Arrhythmia

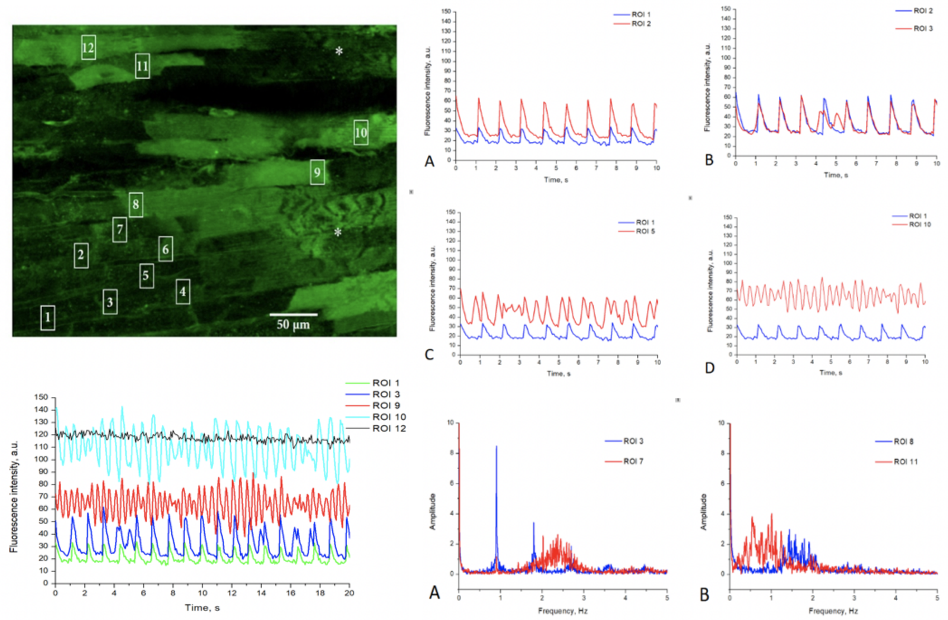

Figure 2: Arrhythmia

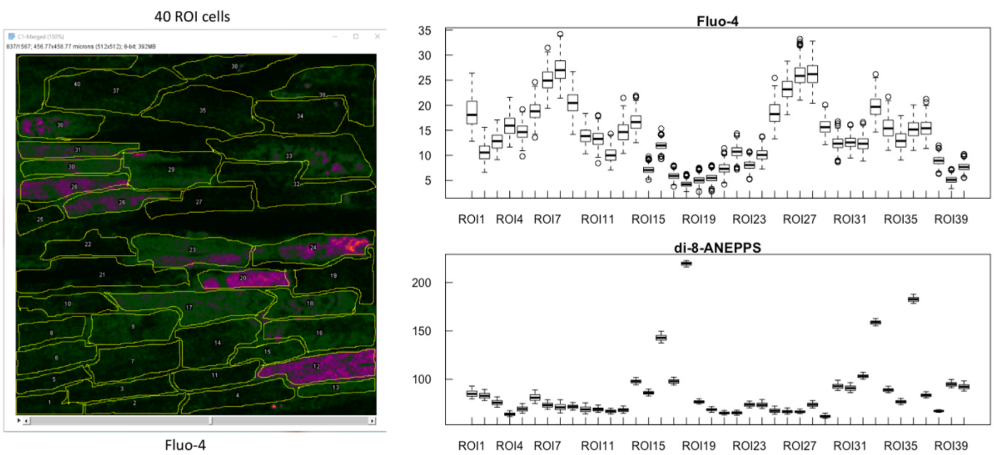

Figure 3: Arrhythmia

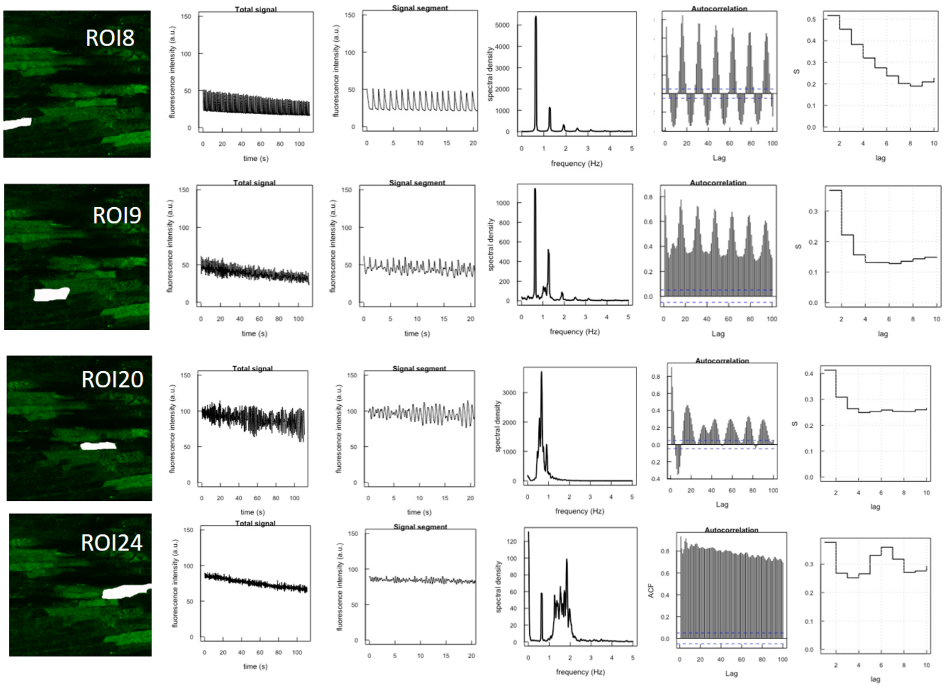

Figure 4: Signal characteristics

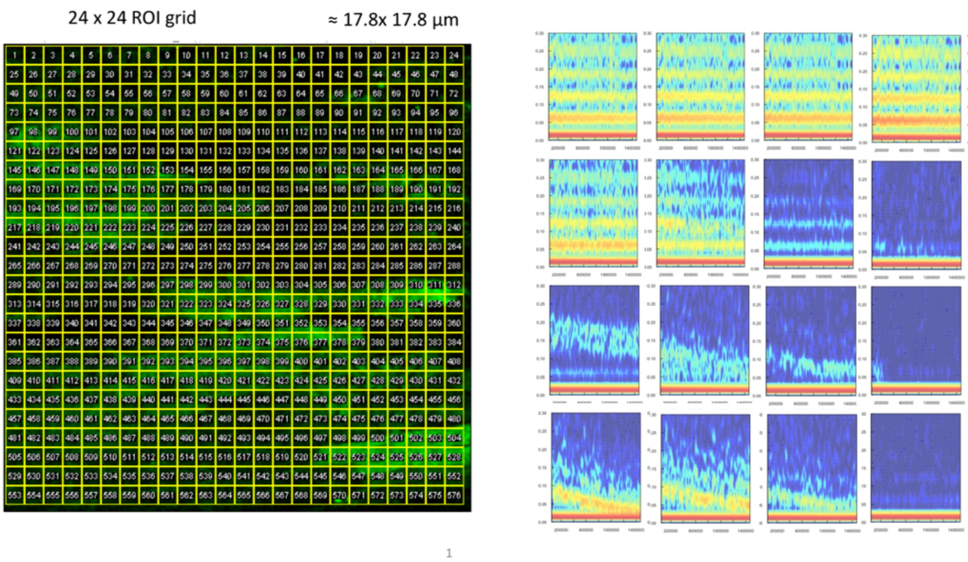

Figure 5: Arrhythmia

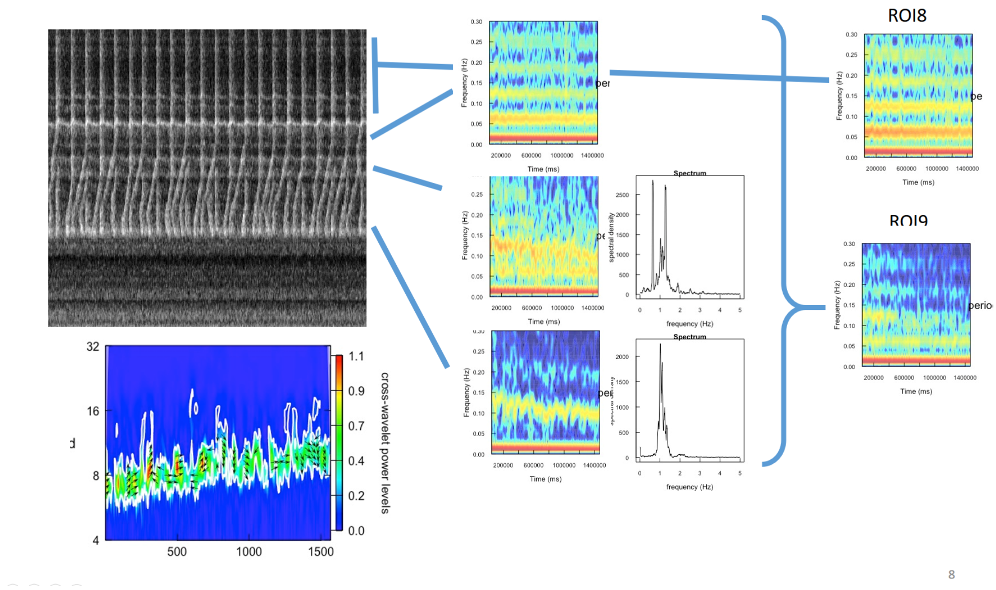

Figure 6: Arrhythmia

boring cells, C - comparison of signals in cells lying at a distance of 100 μ m from each other, D - comparison of signals in cells lying at a distance of 300 μ mfrom each other. The FFT analysis of calcium oscillations showed that in the cardiomyocytes of the perineecrosis boundary zone, as the concentration of Ca2 + increases, the amplitude of normal fluctuations in the concentration of ionized Ca2 + first increases (Figure 11, A), then single calcium waves break the sinus rhythm (Figure 11, B) , then autonomous high-frequency calcium oscillations arise that attenuate, reaching a certain threshold, (Figure 11, Figure 13, Figure 13), after which the cardiomyocytes begin to hypershrink. Such calcium waves can be a source of arrhythmias and contribute to the development of contractile dysfunction in heart diseases.

Fig. 2. Calcium waves in rat myocardium against a background of global calcium release. Optical section of the epicardial region of the ventricular myocardium of the isolated working heart of the rat, painted Di-8-ANEPPS (red) and Fluo-4 (green), combined image. The scale segment is 100 μm. White squares indicate the selected ROI size of 100 μm x 100 μm. Fluorescent fluorescence intensity plots in selected ROI: red line - ROI 01, green line - ROI 02. Measurement of the fluorescence intensity versus time in the myocardium, stained for active mitochondria (red) and free calcium ions (green). The scale segment is 20 μm. Shooting for 25 min, the frame corresponding to a point of 500 seconds is presented. A plot of the fluorescence intensity measured in the frame is plotted against time.

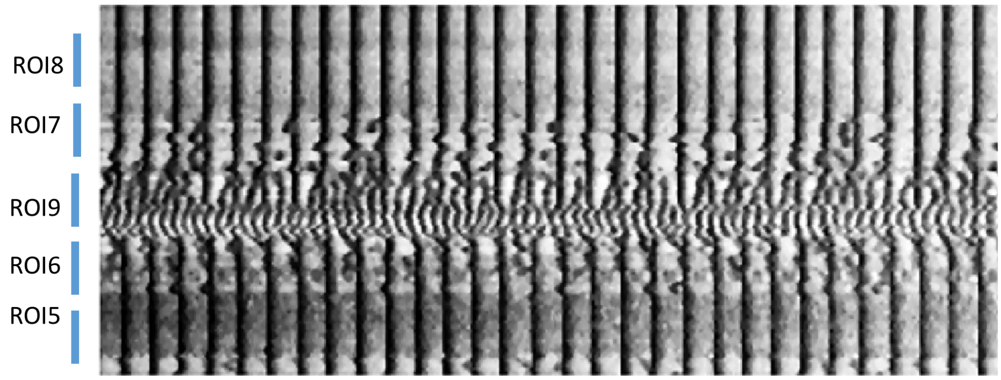

Figure 7: Arrhythmia

Pairwise comparison of the frequencies of calcium waves of cardiomyocytes located in the perinekrozic zone of the ventricular myocardial epicardial region of an isolated working rat heart. A - comparison of signals in neighboring cells, B - comparison of signals in cells lying at a distance of 200 μm from each other Comparison of calcium waves of cardiomyocytes located in the perinekrozic zone of the ventricular myocardial epicardial region of an isolated working rat heart. Plots of fluorescence intensity of Fluo-4 versus time are shown, which are typical for cells located at different stages of damage. The green line is a cell with a normal rhythm; blue line - a cell with a high content of Ca2 + and sinus rhythm disturbances; red line - high-frequency spindle-shaped oscillations; turquoise line - damped oscillations, cell in terminal stage; the black line is a cell in the stage of hypercontraction Calcium waves in cardiomyocytes lying near the necrosis zone. Optical section of the myocardium stained with Fluo-4 (green) and Di-8-ANEPPS (red). On the combined image, the dotted rectangles indicate the selected ROI. The scale segment is 100 μm. On the fluorescence intensity curves of Fluo-4 in the selected ROI, damped oscillations are seen. Total observation time is 90 sec. Optical recording of sinus rhythm in the myocardium. A - Optical sections of the epicardial region of the ventricular myocardium of the isolated working heart of the rat, painted with Di-8-ANEPPS (red) and Fluo-4 (green). B - Fluorescence intensity curves Fluo-4 (black line) and myocardial contractions (red line) versus time. Presented frames are indicated by black arrows. The scale segment is 100 μm.

Calcium waves in rat myocardium against a background of global calcium release. A - Optical sections of the epicardial region of the ventricular myocardium of the isolated working heart of the rat, painted with Di-8-ANEPPS (red) and Fluo-4 (green). B - Plots of fluorescence intensity of Fluo-4 versus time. Presented frames are indicated by black arrows. The scale segment is 100 μm.

Optical section of the myocardium stained with Fluo-4 (green). For comparison, 12 ROIs with a size of 10 μm x 20 μm are selected. The asterisk marks areas with necrotic striation. The scale segment is 10 μm. Graphs of fluorescence intensity of fluo-4 versus time (left column) and the dependence of the frequency of calcium concentration fluctuations on the amplitude (right column) in the selected ROI. Normal vibrations corresponding to sinus rhythm (ROI 1), high-frequency spindle (ROI 10), low-frequency attenuating (ROI 11) oscillations, and a signal characteristic for the cell in the stage of hyper-contraction are presented. Calcium waves in the subepicardial myocardium in Langendorff-perfused rat heart. Fig.1. Cross-sections through image stacks acquired with laser scanning confocal microscopy of ... loaded with Mitochondrial Ca overloading absence of sinus rhythmu Calcium waves in the subepicardial myocardium in Langendorff-perfused rat heart. We found that cardiomyocytes located in the border zone adjacent to the necrosis zone are characterized by an increased content of Ca2 + ions, a reduced mitochondrial potential and contractile activity. Studies were made of the frequency characteristics of calcium waves arising in cardiomyocytes of the border zone. For comparison, 12 cells were selected located next to the necrosis zone (Fig. 9). In each cell, an ROI was determined in which fluorescence fluctuation values of Fluo-4 were measured. The obtained values were processed by the FFT method in the Origin program, some of the frequency characteristics of the calcium waves are shown in Fig. 10 (the data table is presented in the file Fluo-4. When the mitochondria and free Ca2 + ions were stained in the absence of contractile activity and sinus rhythm (inhibition by BDM) in the heart, they were detected as areas of the normal myocardium, characterized by a high $\Delta\ \psi$ and a low value of [Ca2 +] (Fig.2, a, Fig.3, ROI 4-6), and areas of the myocardium, which is in different stages of ischemic damage. An area was identified where, in one field of view of the microscope, it was possible to take readings from cells in successive stages of approach to death. A number of characteristics of the cells were built up, with increasing signs of ischemic damage. For the initial stage of the lesion, groups of cardiomyocytes with a reduced характер and a high value of [Ca2 +] are characteristic (Fig. 2b, Fig. 3, ROI 2-3). In such cells, oscillations of [Ca2 +] (calcium waves) were observed. At further stages of damage in the tissue, foci of necrosis appear, which are noticeable by the appearance of necrotic striation (Fig. 2, c, d). When a normal myocardium section was observed for 25 min, a continuous decrease in the fluorescence intensity of

TMRM was recorded, fluorescence intensity of Fluo-4 first increased for 15 min, and only then began to decrease (Fig. 4). These data are consistent with the notion that as the снижения decreases, the mitochondria begin to accumulate Ca2 +.

По сколько клеток было исследовано в разных областях? Те графики, которые ты даешь, это для отдельных клеток? Если так, надо подробно расписать каждую клетку. Например: образец 1 – интенсивность кальциевого сигнала ???, расположение по отношению к очагу некроза ???, интенсивность МХ ??? и все, что мы еще можем сказать (сократимость, распределение МХ . . .). Сделай это, пожалуйста, для каждого графика. Кроме того, нужно подробное описание каждого графика. Что изменяется конкретно: амплитуда, частота и т.д. Тоже распиши подробно. For the initial stage of damage, groups of cardiomyocytes with an elevated value of [Ca2 +], in which high-frequency calcium waves were observed (Fig. 6), are characteristic. Nascent on the edge of the cell or in its middle, these waves can spread to neighboring cells (Figure 7). With a slight increase in the intracellular calcium concentration, such waves are erased by each subsequent global calcium release (Figure 11, B), and with a strong increase in [Ca2 +] in cardiomyocytes relative to the baseline observed in the normal myocardium, the global calcium release does not interfere with the formation of calcium waves (Fig. 11, B, D). Undoubtedly, the prognostic significance can be the detection of the switching point from the state of the cell, in which global waves can crush pathological, contributing to the restoration of a normal rhythm, to a transition through the "point of no return" when recovery is no longer possible. We found that cardiomyocytes located in the border zone adjacent to the necrosis zone are characterized by an increased content of Ca2 + ions, a reduced mitochondrial potential and contractile activity. Studies were made of the frequency characteristics of calcium waves arising in cardiomyocytes of the border zone. For comparison, 12 cells were selected located next to the necrosis zone (Fig. 9). In each cell, an ROI was determined in which fluorescence fluctuation values of Fluo-4 were measured. The obtained values were processed by the FFT method in the Origin program, some frequency characteristics of the calcium waves are shown in Fig. 10 (the data table is presented in the file Fluo-4 ROI 01-12.xlsx The FFT analysis of calcium oscillations showed that in the cardiomyocytes of the perineecrosis boundary zone, as the concentration of Ca2 + increases, the amplitude of normal fluctuations in the concentration of ionized Ca2 + first increases (Figure 11, A), then single calcium waves break the sinus rhythm (Figure 11, B) , then autonomous high-frequency calcium oscillations arise which, attaining a certain threshold, decay (Figure 11 B, D, Figure 12, Figure 13), after which the cardiomyocytes begin to hyper-shrink. Such calcium waves can be a source of arrhythmias and contribute to the development of contractile dysfunction in heart diseases. The cardiomyocytes adjacent to the necrosis zone were characterized mainly by slow, damped calcium waves with a large amplitude (Fig. 8).

4 DISCUSSION

As was clearly demonstrated (Matsuura et al., 2018), Ischemic myocardial damage manifests itself as a source of calcium waves. We show in this paper, on a model of an isolated rat heart, what a the frequency characteristics of calcium oscillations recorded in the border zone near necrosis. Intracellular calcium accumulation caused by weakening of ATP-dependent mechanisms due to lack of oxygen supply causes foci of high-frequency calcium oscillations that go out of control by sino-atrial thythm.

We assume that such high-frequency activity may cause arrhythmias.

In the ischemic myocardium Ca2+ waves are regarded as arrhythmogenic substrates. To quantitatively image how Ca2+ waves interfere with Ca2+ transients from spontaneous sinus rhythm we used a single-photon confocal laser scanning microscopy in Langendorff-perfused rat hearts. This technique has allowed Intravital imaging visualization of Ca2+ waves propagation at the single-cell level in epicardial cardiomyocytes, avoiding the damage induced by isolation of cardiomyocytes. The effects of hypoxia on oscillations in intracellular calcium concentration ([Ca++]i) were determined in isolated rat heart. The aim was to investigate the frequency characteristics of calcium oscillations arising in the epicardium in response to ischemia Spectral analysis of myocardial analysis of calcium oscillations in rat heart using confocal microscopy was carried out. Optical recording of calcium currents in the rat myocardium during the development of ischemic injury. In cells located at the periphery of the lesion focus, the basal level of calcium remains within normal limits, point-like, prismatic wave sources appear that do not extend to the cell as a whole and are extinguished by a wave of normal ejection. A wave of normal ejection is the result of the work of the pacemaker cells and is accompanied by a synchronous muscle contraction. In cells closer to the lesion focus, the calcium concentration rises. Microtraumas, points of damage are sources of waves. As a result of the hyperscrubbing of ischemic cells, there are gaps between the cardiomyocytes that become the sources of individual transverse waves that cover the whole cell and are able to spread to neighboring cells. As a result of interference of several calcium waves, wave packets arise, the amplitude of which increases as the intracellular concentration of free calcium ions increases. An arrhythmia arises, representing a group of partially damaged and contiguous intact myocardial cells characterized by an elevated concentration of free calcium ions that have their own rhythms of calcium release and muscle contractions and are not affected by pacemaker cells. and during the detachment of the cell the frequency increases spasmodically. Intracellular calcium waves were intensively studied in isolated cardioiocytes by the linescan method (Gyorke, Sunil Kapur). The results obtained revealed the large role of calcium sparks in the nucleation of these waves. Spectral analysis of measure the intensiy of Systolic Ca2+ alternans hypercontracture-indused calcium oscillations interfere with Systolic Ca2+ alternans SR Ca2+ content changes during alternans (Díaz, O'neill, & Eisner, 2004) We assume that high-frequency calcium oscillations arise at the time of cardiomyocyte damage caused by hypercontraction. Since in the course of hypercontraction initial damage can be localized as two adjacent sarcomeres, Propagation of transverse calcium wave along longitudinal axis Such anisotropic protagation of calcium waves was described in 1994 by Engel et al, and velocity of wave propagation rise with temperature. Formation of calcium waves of different type in isolated cardiac myocytes (Ishida, Genka, Hirota, Nakazawa, & Barry, 1999) that this type of calcium waves initiate from stochastic (Izu, Wier, & Balke, 2001) subdiffusive (Chen et al., 2014) Chen et al calcium sparks. This propagation pattern was satisfactorily explained by Finite-element simulations of the three-dimensional cell model, conducted for different intracellular locations of triggering calcium sparks (Tracqui & Ohayon, 2009) we observed for 100 sec Sustained transverse calcium wave patterns in epicard of isolated heart for some time the damaged cardiomyocyte, which has not lost its connection with neighboring cells, can be a source of high-frequency calcium waves, which are transmitted to neighboring cells through gap junctions. Tomoyuki at al using confocal device with simultaneous recording of electrocardiograms demonstrated that Ca2+ waves in Langendorff-perfused rat hearts were completely abolished by ventricular excitation, and that under highly Ca2+ -overloaded conditions Ca2+ waves may occur more frequently and propagate more prevalently to the surrounding cells. Authors suggested that Ca2+ waves play little, if any, pathophysiological role (6,7). Later, it was established that myocardial injury induces Ca2+ waves in the heart (8,9). Baader et al proposed that spatio-temporal summation of changes in membrane potential caused by individual Ca2+ waves may underlie the generation of triggered electrical ectopic impulses (10). In recent years, it has become apparent that myocardial ischemia can cause ventricular arrhythmias and sudden cardiac death. Time series Analysis of oscillation periodicity reveal Wavel coherence analysis of calcium oscillation reveal ... Wavelet transform coherence (WTC) is a method for analyzing the coherence and phase lag between two time series as a function of both time and frequency ((Chang & Glover, 2010)). Here I played with it using the MatLab toolbox provided by Grinsted et al.

Wavelet toolbox is a useful tool to study hyperscanning data. Many recent publications on NIRS hyperscanning use wavelet coherence to quantify the relationship between two interacting brains (e.g. Baker et al 2016, Nozawa et al 2016). You can see more information about wavelet coherence at http://www.alivelearn.net/?p=1169

In the above figure, I plot the wavelet coherence between the two signals in both time and frequency domain. Coherence is kind of correlation. 1 (red) means the two signals are highly correlated and 0 (blue) means no correlation. There are definitely something interesting between the two signals.

First, there is a red band in the period 8 region. As the sampling frequency of the signals is 10Hz, period 8 means 0.8s. This band is originated from heart beating (1Hz) and indicates that the two people's heart beating is highly correlated.

Second, there are some red blobs in the period 64 region. The button pressing is occurring at 6-7s frequency. These blobs indicate that the two people's brain are correlated during button pressing.

So, with wavelet coherence analysis, you can discover something you might not discover with other methods.

In the following examples, I created two time series, x (blue) and y (red) with different properties (phase shift, frequency and amplitude) and run wtc(x,y,'mcc',0) command. Small white noise was added to the time series.

1. Phase shift and angle. A rightward arrow indicates 0 lag; a bottom-right arrow indicates a small lehttp://www.alivelearn.net/?p=1169 Xu Cui

Dissinchrony Alternans Hypoxia Frequency Cardiac Heart imaging Repolarization Propagation Release Measurements Dynamics Changes Information Arrhythmia Arrhythmogenic Ectopic Myocardial alternans Increase Experimental Motion time Mitochondrial Radiation of aberrant signal Noise Oscillations Stochastic calcium Oscillations Phenomenon This resulted in during the repolarization phase, thus further increasing APD and Ca2+ loading. This positive-feedback loop led to EADs and ultimately failure to repolarize. It is possible that the saturating behavior of LCC Ca2+-dependent activation in this model prevents sufficient LCC inhibition required for repolarization in the presence of elevated SR Ca2+ The LCC model also does not incorporate "global" [Ca2+]i sensing , which would inhibit LCC openings in the presence of sustained elevated [Ca2+]i. Future work is needed to understand the contributions of these mechanisms, as they may affect the conditions under which the model exhibits DADs during pacing.The distribution of DADs was controlled by both [Ca2+]i and [Ca2+]SR. This was revealed by the apparent change in the threshold SR Ca2+ load for spontaneous Ca2+

wave formation during pacing (see Fig 3). Elevated diastolic [Ca2+]i increased RyR opening rate and thus perpetuated Ca2+ wave formation at lower SR Ca2+ loads. It also caused more rapid loading of the SR to induce overload. Cellular Ca2+ loading also increased the amplitude of DADs due to the greater number and concurrence of Ca2+ wave nucleation sites, which is in agreement with A significant contribution of this work is that the emergence of sudden arrhythmias can be causally linked to stochastic molecular events. A computationally efficient method was developed to estimate the probability of extreme DADs. An important assumption of this method is that the spontaneous Ca2+ release events in neighboring cells are decoupled. It is known that membrane depolarization increases the frequency of Ca2+ waves by reducing NCX-mediated Ca2+ efflux and thus promoting Ca2+ waves due to increased intracellular [Ca2+] (Walker, Gurev, Rice, Greenstein, & Winslow, 2017). In the present study we visualized precise [Ca2+]i dynamics of atrial myocytes in the perfused rat heart. By using the innovative in situ rapid confocal imaging system we constructed, we found that atrial appendage in Langendorff-perfused rat heart has a propensity to show spatiotemporally non-uniform [Ca2+]i dynamics on systole especially during high-frequency excitation. According to our [Ca2+]i dynamics studies to date [9, 11, 25], such nonuniformity in the Ca2+ transients was not predominantly observed in intact ventricles, and the observed features in the atrial [Ca2+]i dynamics would partly be related to the structural difference, i.e., paucity of t-tubules. In principle, individual atrial myocytes in the perfused hearts showed spatiotemporally uniform [Ca2+]i dynamics with frequency-dependent abbreviation of Ca2+-transient durations, a confirmation of the atria being a functional syncytium (Fig. 2). However, even under apparently intact Langendorff perfusion, individual myocytes often exhibited spatially non-uniform [Ca2+]i dynamics, e.g., cluster-like rises of [Ca2+]i, wave-like propagation of [Ca2+]i, and beatto- beat variability of durations and amplitude alternans of Ca2+ transients, all of which emerged on excitation instead of uniform Ca2+ transients (Figs. 3 and 4). (Jiang, Tanaka, Matsuyama, Yamaoka, & Takamatsu, 2014), (Aguirre, Vinegoni, Sebas, & Weissleder, 2014)

Analysis of calcium alternans in ischemic condition calcium overloading cardiac function. spectrum

References

Aguirre, A. D., Vinegoni, C., Sebas, M., & Weissleder, R. (2014). Intravital imaging of cardiac function at the single-cell level. *Proceedings of the*

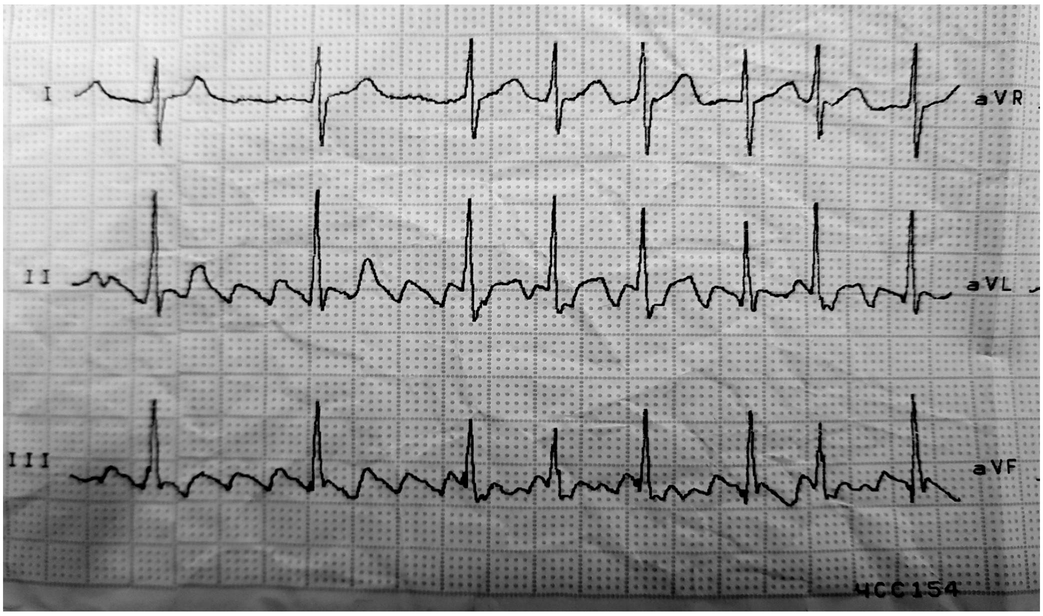

Figure 8: Arrhythmia

National Academy of Sciences, *111*(31), 11257–11262.

Chang, C., & Glover, G. H. (2010). Time–frequency dynamics of resting-state brain connectivity measured with fmri. *Neuroimage*, *50*(1), 81–98.

Chen, W., Wang, R., Chen, B., Zhong, X., Kong, H., Bai, Y., ... others (2014). The ryanodine receptor store-sensing gate controls ca 2+ waves and ca 2+-triggered arrhythmias. *Nature medicine*, *20*(2), 184.

Díaz, M. E., O'neill, S. C., & Eisner, D. A. (2004). Sarcoplasmic reticulum calcium content fluctuation is the key to cardiac alternans. *Circulation research*, *94*(5), 650–656.

Hama, T., Takahashi, A., Ichihara, A., & Takamatsu, T. (1998). Real time in situ confocal imaging of calcium wave in the perfused whole heart of the rat. *Cellular signalling*, *10*(5), 331–337.

Ishida, H., Genka, C., Hirota, Y., Nakazawa, H., & Barry, W. H. (1999). Formation of planar and spiral ca2+ waves in isolated cardiac myocytes. *Biophysical journal*, *77*(4), 2114–2122.

Izu, L. T., Wier, W. G., & Balke, C. W. (2001). Evolution of cardiac calcium waves from stochastic calcium sparks. *Biophysical journal*, *80*(1), 103–120.

Jiang, Y., Tanaka, H., Matsuyama, T.-a., Yamaoka, Y., & Takamatsu, T. (2014). Pacing-induced non-uniform ca2+ dynamics in rat atria revealed by rapid-scanning confocal microscopy. *Acta histochemica et cytochemica*, *47*(2), 59–65.

Kockskämper, J., & Blatter, L. A. (2002). Subcellular ca2+ alternans represents a novel mechanism for the generation of arrhythmogenic ca2+ waves in cat atrial myocytes. *The Journal of physiology*, *545*(1), 65–79.

Matsuura, R., Miyagawa, S., Fukushima, S., Goto, T., Harada, A., Shimozaki, Y., ... others (2018). Intravital imaging with two-photon microscopy reveals cellular dynamics in the ischeamia-reperfused rat heart. *Scientific reports*, *8*(1), 15991.

Minamikawa, T., Cody, S. H., & Williams, D. A. (1997). In situ visualization of spontaneous calcium waves within perfused whole rat heart by confocal imaging. *American Journal of Physiology-Heart and Circulatory Physiology*, *272*(1), H236–H243.

Nayler, W. G. (1981). The role of calcium in the ischemic myocardium. *The American journal of pathology*, *102*(2), 262.

Roesch, A., & Schmidbauer, H. (2014). Waveletcomp: Computational wavelet analysis. *R package version*, *1*.

Shen, A. C., & Jennings, R. B. (1972a). Kinetics of calcium accumulation in acute myocardial ischemic injury. *The American journal of pathology*, *67*(3), 441.

Shen, A. C., & Jennings, R. B. (1972b). Myocardial calcium and magnesium in acute ischemic injury. *The American journal of pathology*, *67*(3), 417.

Takamatsu, T. (2008). Arrhythmogenic substrates in myocardial infarct. *Pathology international*, *58*(9), 533–543.

Team, R. C., et al. (2014). R: A language and environment for statistical computing. *R*.

Tracqui, P., & Ohayon, J. (2009). An integrated formulation of anisotropic force–calcium relations driving spatio-temporal contractions of cardiac myocytes. *Philosophical Transactions of the Royal Society of London A: Mathematical, Physical and Engineering Sciences*, *367*(1908), 4887–4905.

Walker, M. A., Gurev, V., Rice, J. J., Greenstein, J. L., & Winslow, R. L. (2017). Estimating the probabilities of rare arrhythmic events in multiscale computational models of cardiac cells and tissue. *PLoS computational biology*, *13*(11), e1005783.